THE JOURNAL OF BIOLOGICAL CHEMISTRY
Vol. 280, No. 23, Issue of June 10, pp. 22335–22342, 2005

Printed in U.S.A.

Mind Bomb-2 Is an E3 Ligase for Notch Ligand*[S]

Received for publication, February 11, 2005, and in revised form, April 4, 2005
Published, JBC Papers in Press, April 11, 2005, DOI 10.1074/jbc.M501631200

Bon-Kyoung Koo‡, Ki-Jun Yoon‡, Kyeong-Won Yoo§, Hyoung-Soo Lim‡, Ran Song‡, Ju-Hoon So§, Cheol-Hee Kim§¶, and Young-Yun Kong‡‖

From the ‡Division of Molecular and Life Sciences, Pohang University of Science and Technology, Pohang, Kyungbuk, 790-784 South Korea and the §Department of Biology, Chungnam National University, Daejeon 305-764, South Korea

The zebrafish gene, *mind bomb* (*mib*), encodes a protein that positively regulates of the Delta-mediated Notch signaling. It interacts with the intracellular domain of Delta to promote its ubiquitination and endocytosis. In our search for the mouse homologue of zebrafish *mind bomb*, we cloned two homologues in the mouse genome: a mouse orthologue (mouse *mib1*) and a paralogue, named *mind bomb-2* (*mib2*), which is evolutionarily conserved from *Drosophila* to human. Both Mib1 and Mib2 have an E3 ubiquitin ligase activity in their C-terminal RING domain and interact with *Xenopus* Delta (XD) via their N-terminal region. Mib2 is also able to ligate ubiquitin to XD and shift the membrane localization of Delta to intracellular vesicles. Importantly, Mib2 rescues both the neuronal and vascular defects in the zebrafish *mib*^{ta52b} mutants. In contrast to the functional similarities between Mib1 and Mib2, *mib2* is highly expressed in adult tissues, but almost not at all in embryos, whereas *mib1* is abundantly expressed in both embryos and adult tissues. These data suggest that Mib2 has functional similarities to Mib1, but might have distinct roles in Notch signaling as an E3 ubiquitin ligase.

The Notch signaling pathway is an evolutionarily conserved intercellular signaling mechanism, in which both the ligands and receptors are type 1 transmembrane proteins, thus restricting the Notch pathway to the regulation of interactions between physically adjacent cells (1–3). To date, four Notch receptors and five ligands (Delta-like (Dll)-1, -3, and -4, and Jagged (Jag) 1 and 2) have been described in mammals. The interactions between these Notch receptors and ligands are essential for a wide range of developmental cell-to-cell interactions. When ligand-receptor interactions induce the sequential proteolytic cleavage events that release the intracellular domain of Notch receptor from the cell membrane, the Notch signaling pathway is activated (4–6). In the nucleus, the intracellular domain of Notch receptor forms a complex with CSL (CBF1/RBP-Jκ, Su(H), Lag-1). This complex is a transcriptional activator, which induces the expression of genes encoding Hairy/Enhancer-of-split (HES)-related proteins, which inhibit the basic helix-loop-helix transcription factors (7, 8). Many components of the Notch signaling pathway in *Drosophila* were originally identified by mutants that confer a similar neurogenic phenotype in early embryos. The mutations of these genes, such as *notch, delta*, *E*(*SPL*), *mastermind*, and *neuralized*, result in an increase of neural cells at the expense of epidermal structures (9).

The signaling by Notch receptors involves three successive cleavages: the S1 cleavage in the trans-Golgi network by Furin-like proteases, the ligand-dependent extracellular S2 cleavage by metalloproteinases, and the intramembraneous S3 cleavage by γ-secretase complexes to release the active intracellular domain of Notch receptor (10). In the signaling cell, Delta-Notch interactions result in the endocytosis of Delta, which carries along the bound Notch extracellular domain, and the endocytosis-defective Delta mutants have reduced signaling capacity. The ligand-dependent extracellular S2 cleavage of Notch receptor is coupled to the trans-endocytosis of the Notch extracellular domain into the ligand expressing/signal sending cell (2). To date, there are two candidate genes, Neuralized (Neur) and Mib, which promote the ubiquitination and endocytosis of Notch ligands. Recently, Itoh *et al.* (11) reported that Mib promotes the ubiquitination and endocytosis of zebrafish DeltaD and DeltaB.

Although Mind bomb and Neur might be key regulators in the endocytosis of Delta for the activation of Notch receptors, the molecular diversity of the vertebrate genes encoding five Notch ligands (Dll1, Dll3, Dll4, Jag1, and Jag2) and four Notch receptors (Notch1–4) in mammals suggests that there might be an additional E3 ubiquitin ligase that regulates Notch ligands. Indeed, all of these ligands have unique expression patterns, and the knock-out mice for each gene display a distinct phenotype. In parallel with the diversity of the ligands, more complex endocytic machinery might exist as well (12–20). In our search for the mouse Mind bomb homologue, we found one Mind bomb orthologue (Mib1) and one Mind bomb paralogue, Mind bomb-2 Mib2 (AY974090) skeletrophin (21). Here we show that Mib2 is another E3 ubiquitin ligase that ubiquitinates the Notch ligand, Delta, and promotes its endocytosis. We propose that Mib2 might be an important E3 ubiquitin ligase for Delta in the Notch signaling pathway.

MATERIALS AND METHODS

Cloning of the Mouse mib2 Gene and Generation of Mutations in the Mib2 RING Finger Domain—PCR was carried out using mouse brain cDNA as the template and oligonucleotide primers designed to obtain the open reading frame of the mouse *mib2* gene. The PCR for *mib2*

* This work was supported by Vascular System Research Center Grant R11-2001-090-03001-0 from KOSEF, Basic Research Program of the Korea Science & Engineering Foundation Grant R02-2003-000-10057-0), the 21C Frontier Functional Human Genome Project from Ministry of Science and Technology of Korea Grant FG04-22-05), and Molecular and Cellular BioDiscovery Research Program Grant M1-0106-01-0001 from the Ministry of Science and Technology, South Korea. The costs of publication of this article were defrayed in part by the payment of page charges. This article must therefore be hereby marked "*advertisement*" in accordance with 18 U.S.C. Section 1734 solely to indicate this fact.

The nucleotide sequence(s) reported in this paper has been submitted to the GenBank™/EBI Data Bank with accession number(s) AY974090 and AY974091.

[S] The on-line version of this article (available at http://www.jbc.org) contains Fig. S1.

¶ To whom correspondence may be addressed. Fax: 82-42-822-9690; E-mail: zebrakim@cnu.ac.kr.

‖ To whom correspondence may be addressed. Fax: 82-54-279-2199; E-mail: ykong@postech.ac.kr.

yielded a product of about 2750 bp, which was cloned into the hemagglutinin (HA)[1]-tagged pcDNA vector (Invitrogen) or the pEGFPN3 vector (Clontech). The *mib2* mutants with mutations in the RING finger domain were generated using DpnI-mediated site-directed mutagenesis. All of the cloned cDNA vectors were confirmed by restriction enzyme digestion and DNA sequencing.

Northern Blot Analysis—Two probes were generated to detect the N- and C-terminal regions of Mib2. The PCR primers for the N-terminal probe (5′-probe) were mib2NL (CAGGTCGTGTGGTGGACAT) and mib2NR (GCTGTTGTGCTTGGTGAGAG). The PCR primers for the C-terminal probe (3′-probe) were mib2CL (GGTCGCTGTGATGTGAATGT) and mib2CR (CTGCCTGTCGTCCCTGAAG). For the expression analysis in the mouse adult tissues, the Mouse Multiple Tissue Northern blot (Clontech) was hybridized with both probes.

Whole Mount in Situ Hybridization—Details of the RNA *in situ* hybridizations with zebrafish embryos were described for the various probes: *huC* (22), *flt4* (23), and *ephrinB2a* (23). To detect the β-galactosidase co-injected with the synthesized mRNAs, the embryos were fixed in 4% paraformaldehyde in phosphate-buffered saline at 4 °C for 1 h and stained in 5-bromo-4-chloro-3-indolyl-β-D-galactopyranoside (X-gal) staining buffer. *In situ* probes for mouse *mib1* and *mib2* were generated from HindIII-cleaved pcDNA-Mib1 and pcDNA-Mib2 expression vectors by Sp6 RNA polymerase (Fermentas). *In situ* probes for zebrafish *mib1* and *mib2* were cloned into pBluescript vectors (Invitrogen) and synthesized with SalI-cleaved vectors by T7 RNA polymerase (Fermentas). The PCR primers for the zebrafish *mib1* probe were z-mib1L (AGCAGACGGCATTACACCTT) and z-mib1R (TACCTTTCCCTCCACAGCAC). The PCR primers for the zebrafish *mib2* probe were z-mib2L (ACATCAACATCCGCAACAAC) and z-mib2R (CGCTCCTCCATCTGTCTGTA).

Cell Culture and Transfections—HEK-293A or HeLa cells were grown in Dulbecco's modified Eagle's medium containing 10% fetal bovine serum and antibiotics. Cells were transfected with appropriate amounts of plasmid DNA using Lipofectamine Plus (Invitrogen). Cells were harvested 24–48 h after transfection in 1 ml of lysis buffer (10 mM Tris (pH 7.5), 150 mM NaCl, 5 mM EDTA) containing protease inhibitors (Roche). The lysates were sonicated several times, and the insoluble debris was removed by centrifugation. Aliquots of the supernatants, containing 15–40 μg of protein, were separated on a polyacrylamide gel and transferred to a polyvinylidene difluoride membrane. The membrane was blotted with the primary antibody of interest and a secondary antibody. To detect the immunoreactive bands, ECL plus was used (Amersham Biosciences).

Zebrafish Maintenance and mRNA Microinjections—Zebrafish were raised and maintained under standard conditions. The zebrafish mutant mib^{ta52b} was used as the *mib1* mutant. The mouse *mib2* cDNA was subcloned into the pCS2+ vector and the sense RNA encoding full-length mouse *mib2* was transcribed *in vitro* using the SP6 Message Machine (Ambion, Austin, TX). The synthesized *mib2* mRNA was microinjected into one-cell or two-cell stage zebrafish embryos. The amount of mRNA (~100 pg) injected into the embryos was visually estimated from the injection volume.

Immunoprecipitation—HEK-293A cells, transfected with 4 μg of plasmid DNA per 10-cm plate, were resuspended in IP buffer (50 mM HEPES/NaOH (pH 7.5), 3 mM EDTA, 3 mM $CaCl_2$, 80 mM NaCl, 1% Triton X-100, 5 mM dithiothreitol). After the cells were disrupted, the extracts were centrifuged to remove the debris. The supernatants were cleared using protein A/G Plus-agarose (Santa Cruz Biotechnology) at 4 °C for 1 h. The indicated proteins were immunoprecipitated by the addition of protein A/G beads pre-complexed with an anti-HA antibody or anti-Myc antibody at 4 °C for 8 h. The immune complexes bound to the protein A/G beads were washed with IP buffer and boiled in 2× SDS gel loading buffer, and the eluted proteins were electrophoresed on a polyacrylamide gel. Immunoreactive proteins were analyzed by immunoblotting with an anti-Myc antibody (Santa Cruz Biotechnology) or anti-Ub antibody (P4D1; Santa Cruz Biotechnology) followed by either a goat anti-mouse horseradish peroxidase-conjugated antibody (Promega) or an anti-HA horseradish peroxidase-conjugated antibody (Santa Cruz Biotechnology).

In Vitro and in Vivo Ubiquitination Assays—*In vitro* ubiquitination assays were modified from those previously described (11). Briefly, the reactions contained ubiquitin-activating enzyme (E1; Calbiochem), glutathione *S*-transferase (GST)-tagged ubiquitin-conjugating enzyme Ubc5a (E2; Calbiochem), N-terminal His-tagged ubiquitin (Sigma), and ATP (2 mM). The purified GST-fused Mib1 and Mib2 RING and their mutants were added to the reactions. After incubation at room temperature, the reactions were analyzed by Western blotting to detect the ubiquitinated proteins.

To detect the ubiquitination activity *in vivo*, HEK-293A cells were transfected with 4 μg of plasmid DNA per 10-cm plate. MG132 (2 μM) was added 24 h after transfection, and the cells were harvested 24 h later. The lysates were prepared in RIPA buffer (2 mM Tris-Cl (pH 7.5), 5 mM EDTA, 150 mM NaCl, 1% Nonidet P-40, 1% deoxycholate, 0.025% SDS), and clarified by centrifugation. The supernatants were immunoprecipitated and the immunoreactive proteins were detected with an anti-ubiquitin antibody (P4D1; Santa Cruz Biotechnology) followed by an anti-mouse horseradish peroxidase-conjugated antibody (Promega).

Subcellular Localization Analysis—HeLa cells were transfected with various plasmids. At 24 h post-transfection, the cells were washed in phosphate-buffered saline and fixed in 4% paraformaldehyde with 3% sucrose for 30 min at 4 °C. The fixed cells were incubated in blocking solution (3% skim milk and 0.1% Triton X-100 in phosphate-buffered saline) overnight at 4 °C, and then stained with mouse anti-Myc and anti-HA antibodies (Santa Cruz Biotechnology) in 3% skim milk in phosphate-buffered saline for 1 h at room temperature. Subsequently, the cells were incubated with an anti-mouse antibody conjugated with TRITC for 30 min at room temperature. The cells were washed and then stained with Hoechst (10 μg/ml) for 2 min. After three washes, the cells were mounted on glass slides and analyzed with a Zeiss fluorescent microscope. All images were collected on a Zeiss AxioCam HRc camera.

RESULTS

Mib2 Is a Mib1 Paralogue—Zebrafish Mib1 is a E3 ubiquitin ligase that is an essential component of Notch signaling in lateral inhibition (11). By searching the EST and genomic databases, we found that the human and mouse genomes contained one *mib* orthologue (*mib1*, AY974091) and one *mib* paralogue, *mind bomb-2* (*mib2*, AY974090). To investigate the function of Mib2, its cDNA was cloned and amplified through reverse transcriptase-PCR from mouse brain and thymus RNA. During sequence confirmation, we found that it has several splicing variants. To clone the dominant form among the splicing variants, we compared the restriction enzyme digestion patterns and the sequences of independently subcloned cDNAs. From this comparison, we concluded that there were two major splicing variants. We also amplified the variable region of these two variants to determine the most abundant form in the various tissues. One of the two variants represented about 70% of the total *mib2* transcripts, with slight differences in the various tissues. We also found that part of the *mib2* amino acid sequences differs from the sequence of *skeletrophin* in the NCBI database. However, extensive confirmations of the different regions revealed that our sequence is correct (Fig. 1*A*).

Mouse Mib1 and Mib2 have 36% identity and 52% similarity in their amino acid sequences, and they also have remarkable resemblance in their domain organization (Fig. 1, *A* and *B*). Mib2 has two herc2/mib domains, one ZZ zinc finger, one mib repeat, ankyrin repeats, and two RING domains (11). All of these domains are organized in a similar manner as compared with those of Mib1. Mib2 appears to be evolutionarily conserved from *Drosophila* to human (data not shown). Northern blot analyses using 5′- and 3′-probes revealed a 4.4-kb *mib2* transcript, which could include its open reading frame (~2.8-kb). We could not distinguish the splicing variants, which might be because of a small difference in the nucleotide length. *mib2* was highly expressed in the heart, brain, liver, and kidney (Fig. 1*C*), whereas *mib1* was highly expressed in testis (data not shown). The different expression patterns of these two genes suggest a distinct role of *mib2 in vivo* as compared with those of *mib1*.

Mib2 Is an E3 Ubiquitin Ligase—Zebrafish Mib1 has an E3 ubiquitin ligase activity with Delta, both *in vitro* and *in vivo* (11). Based on the sequence homology and the similar domain

[1] The abbreviations used are: HA, hemagglutinin; E1, ubiquitin-activating enzyme; E2, ubiquitin carrier protein; E3, ubiquitin-protein isopeptide ligase; GST, glutathione *S*-transferase; mib, mind bomb; DA, dorsal artery; TRITC, tetramethylrhodamine isothiocyanate.

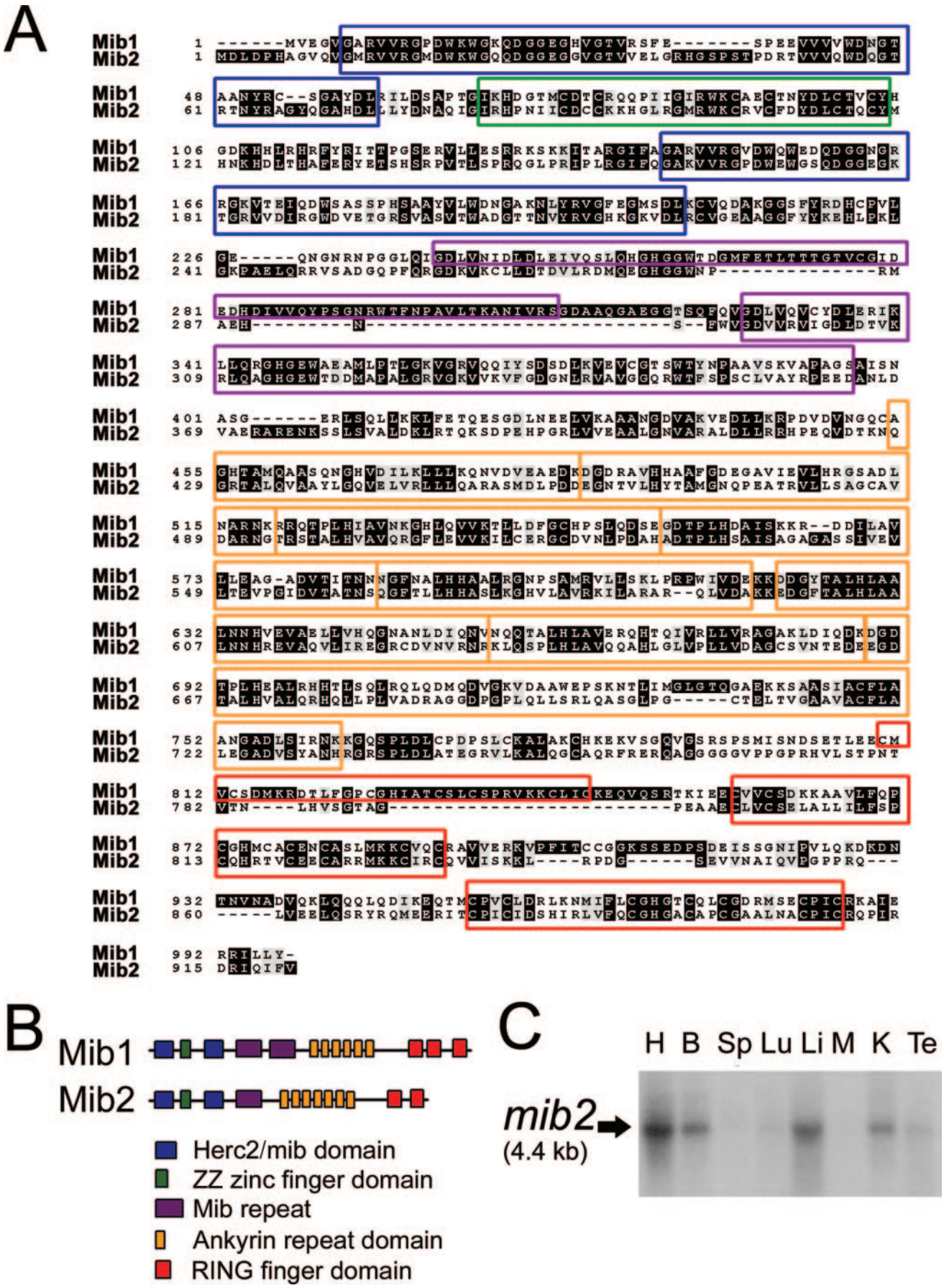

FIG. 1. **Cloning of mouse mind bomb-1 (*Mib1*) and -2 (*Mib2*).** *A*, the amino acid sequences of mouse Mib1 and Mib2. The *colored boxes* indicate the domains depicted in *B*. *B*, structures of the Mib1 and Mib2 proteins with predicted domains. *C*, Northern blot analysis of Mib2 expression in adult mouse tissues. *H*, heart; *B*, brain; *Sp*, spleen; *Lu*, lung; *Li*, liver; *M*, skeletal muscle; *K*, kidney; *T*, testis.

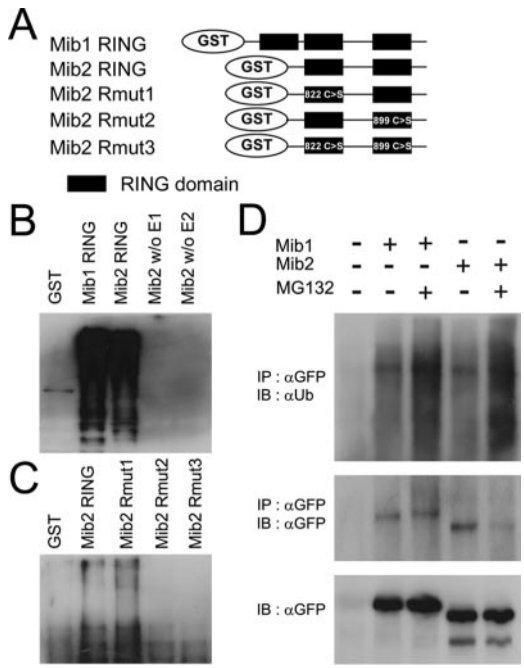

FIG. 2. **Mib2 is an E3 ubiquitin ligase.** *A*, schematic drawing of Mib2 RING constructs. *Boxes* indicate RING finger domains. *B*, E1- and E2-dependent self-ubiquitination by the Mib2 RING domain. GST fusion proteins of Mib2 RING were incubated in a reaction mixture in the presence or absence of E1 and E2 (*Ubc5a*). GST and GST-Mib1 RING were used as negative and positive controls, respectively. Ubiquitination was detected by an anti-ubiquitin antibody. *C*, the second RING finger domain-dependent self-ubiquitination. The Mib2 RING mutants (Rmut1–3) depicted in *A* were assayed as in *B*. *D*, self-ubiquitination by Mib2 *in vivo*. HEK-293A cells were transfected with plasmids encoding full-length Mib2-GFP in the presence or absence of MG132. At 36 h post-transfection, whole cell lysates were immunoprecipitated with an anti-GFP (*B2*) antibody and immunoblotted with an anti-Ub (*P4D1*) antibody. Full-length Mib1-GFP was used as a positive control. *IB*, immunoblot.

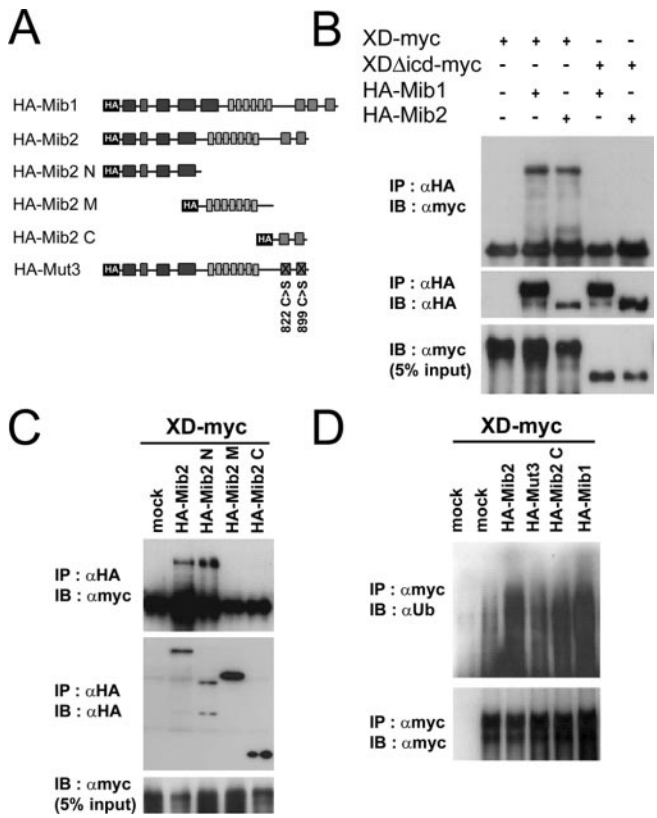

FIG. 3. **Mib2 interacts with *Xenopus* Delta ligand.** *A*, schematic drawing of HA-tagged Mib2 constructs. *B* and *C*, interaction between Mib2 and *Xenopus* Delta (*XD*) through the C-terminal cytoplasmic domain of XD and the N-terminal domain of Mib2. HEK-293A cells were co-transfected with various plasmid constructs. Cell lysates were immunoprecipitated (*IP*) with an anti-HA antibody and detected with an anti-Myc antibody. The *top panels* show immunoprecipitations of XD by the Mib2 constructs, and the *middle* and *bottom panels* are blots showing the expression of the Mib2 and Delta constructs, respectively, in cell lysates. Mib1 was used as a positive control. *D*, ubiquitination of XD by the various Mib2 constructs. HEK-293A cells were co-transfected with various plasmid constructs. Cell lysates were immunoprecipitated with an anti-Myc antibody and detected with an anti-Ub antibody. The *top panel* shows the ubiquitination of XD by Mib2 constructs, and the *bottom panel* is a blot showing the expression of the XD construct in cell lysates. Mib1 was used as a positive control. *IB*, immunoblot.

organization, we speculate that Mib2 might have a similar biochemical activity. To test the intrinsic ubiquitin ligase activity of the Mib2 RING finger *in vitro*, GST-Mib2 RING finger fusion proteins were incubated with ubiquitin-activating enzyme (E1) and ubiquitin-conjugating enzyme (E2), ubiquitin, and ATP. The presence of ubiquitinated substrates was detected by Western blotting. As expected, a typical reaction mixture containing the RING finger domain from Mib1 resulted in a smear of high molecular weight polyubiquitinated substrates (Fig. 2*B*, *lane 2*), whereas a similar reaction containing GST was devoid of such activity (Fig. 2*B*, *lane 1*). When GST-Mib2 RING was tested in this assay, we observed robust ubiquitination in an E1 and E2 (UbcH5a) dependent manner (Fig. 2*B*, *lanes 3–5*), indicating that Mib2 RING possesses an E3 ubiquitin ligase activity.

Because Mib2 contains two RING finger domains, we tested which domain is necessary for the E3 ubiquitin ligase activity. We generated three RING mutant proteins that have a mutation in the first RING domain (Rmut1; C822S), the second RING domain (Rmut2; C899S), and both domains (Rmut3; C822S and C899S). In the mutant proteins containing a mutation in the second RING domain, the ubiquitination activity was strongly diminished (Fig. 2*C*, *lanes 4* and *5*), whereas the mutation in the first RING domain did not affect the self-ubiquitination activity, indicating that the second Mib2 RING is directly responsible for the ubiquitin ligation in this reaction.

To test the self-ubiquitination activity of Mib2 *in vivo*, HEK-293A cells were transfected with plasmids encoding full-length Mib2-GFP and Mib1-GFP. At 36 h post-transfection, whole cell lysates were immunoprecipitated with an anti-GFP (B2) antibody and immunoblotted with an anti-Ub (P4D1) antibody. Both Mib1 and Mib2 displayed increased levels of ubiquitination activity as compared with the mock-transfected control, and ubiquitination was dramatically increased in the presence of the proteosome inhibitor, MG132 (Fig. 2*D*, *lanes 3* and *5*), suggesting the proteosomal degradation of these ubiquitinated proteins.

Mib2 Interacts with Xenopus Delta Ligand—Both zebrafish Mib1 and *Drosophila* Neur interact with Delta, and they ubiquitinate it to target it to the cellular endocytic machinery (11, 24, 25). To test the possibility that Mib2 also interacts with and ubiquitinates Delta, HA-tagged Mib2 (HA-Mib2) was co-transfected with either myc-tagged *Xenopus* Delta (XD-myc) or *Xenopus* Delta without its intracellular domain (XD-Δicd-myc) in HEK-293A cells. HA-Mib2 was immunoprecipitated with an anti-HA antibody and immunoblotted with an anti-Myc antibody to detect the co-immunoprecipitation of Myc-tagged ligands. The results showed that both Mib1 and Mib2 interact with XD, but not with XD-Δicd (Fig. 3*B*). These data indicate that Mib2 binds to XD and that the intracellular domain of Delta ligand is essential for the interaction with Mib2.

To identify the region of Mib2 that interacts with Delta

ligand, XD-myc was co-transfected with HA-Mib2 or truncated forms of Mib2: the N-terminal region (amino acids 1–427), the middle region (amino acids 319–785), and the C-terminal region (amino acids 778–921) (Fig. 3*A*). All of the Mib2 forms were immunoprecipitated with an anti-HA antibody and immunoblotted with an anti-Myc antibody to detect the co-immunoprecipitation of XD-myc. Both full-length Mib2 and the truncated protein that included the N-terminal region were co-immunoprecipitated with XD-myc (Fig. 3*C*, *lanes 2* and *3*). Taken together, these results indicate that Mib2 interacts with the intracellular domain of Delta through its N-terminal region.

Mib2 Ubiquitinates Xenopus Delta Ligand—Zebrafish Mib1 interacts with Delta through its N-terminal and middle regions, and the Zebrafish Mib1 RING finger domain is responsible for the ubiquitination of Delta (11). Because Mib2 also showed comparable activities in terms of self-ubiquitination and interaction with Delta, we examined whether it promotes ubiquitination of Delta. Accordingly, XD-myc and the candidate E3 ubiquitin ligases were co-transfected in HEK-293A cells. XD-myc was immunoprecipitated by an anti-Myc antibody, and the presence of ubiquitinated XD-myc was detected with an anti-Ub antibody. The ubiquitination of XD-myc was enhanced in the presence of both HA-Mib2 and HA-Mib1 (Fig. 3*D*, *lanes 3* and *6*). As expected, Mib2 mutant 3, which has mutations in the first and second RING domains (C822S and C899S), showed a basal level of ubiquitination, and the C-terminal region of Mib2, which does not bind Delta, showed a relatively low level of ubiquitination (Fig. 3*D*, *lanes 4* and *5*). From these data, we concluded that Mib2 interacts with and ubiquitinates Delta through its N-terminal region and RING finger domain, respectively.

Mib2 has two RING finger domains, and the second Mib2 RING is directly responsible for self-ubiquitination (Fig. 2*C*). To test whether both RING finger domains are essential for the ubiquitination of Delta, Mib2 mutant proteins with point mutations in their RING finger domain (Mut1, 2, and 3 as previously described) were co-transfected with XD-myc. Unexpectedly, none of these mutants ubiquitinated XD-myc *in vivo* (Fig. 4*B*, *lanes 3–5*), despite the self-ubiquitination activity of the Mib2 RING mutant (Rmut1; C822S) *in vitro* (Fig. 2*C*, *lane 3*). These data indicate that both RING domains in Mib2 are essential for proper ubiquitination of its substrate, Delta.

Mib2 Changes the Subcellular Localization of Xenopus Delta Ligand—To characterize the subcellular localization of Mib2, we used subcellular markers that distinguish the intracellular subcompartments (26). HeLa cells transfected with Mib2-GFP were stained with specific antibodies for the endogenous markers, EEA1 (early endosome antigen 1; early endosome), M6PR (mannose 6-phosphate receptor; late endosome), or HA-Hrs (hepatocyte responsive serum phosphoprotein; ubiquitinated cargo). Interestingly, Mib2-GFP co-localized with the early endosomal marker, EEA1, but not with M6PR or Hrs (supplemental materials Fig. 1). Taken together, these results indicate that Mib2 is an endosomal protein localized in the early endosomal compartments.

In general, the ubiquitination of membrane proteins serves as a tag for endocytosis or for lysosomal targeting (27, 28). To test whether Mib2 promotes the endocytosis of Delta, we co-expressed XD-myc along with Mib2-GFP in HeLa cells. When Mib2-GFP alone was expressed, it was localized in the cytoplasm as punctate structures (Fig. 4*C*, *b* and *b′*). XD-myc alone was expressed on the plasma membrane (Fig. 4*C*, *a* and *a′*). In contrast, when both XD-myc and Mib2-GFP were co-expressed, XD-myc expression on the cell surface was decreased, and it accumulated in the cytoplasm as a vesicular structure, where it

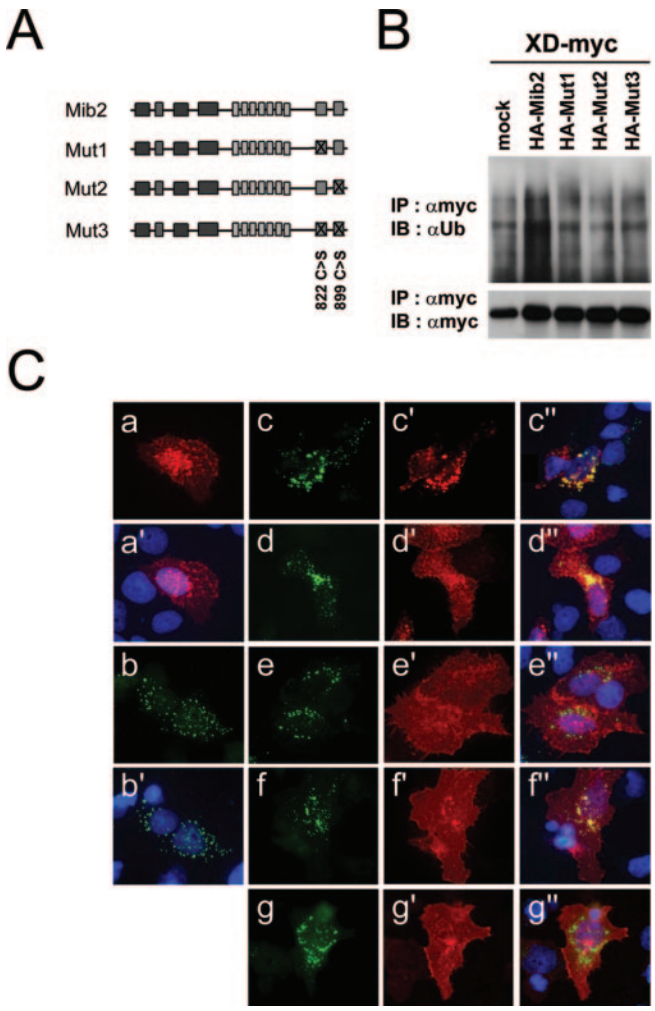

FIG. 4. **Mib2 changes the subcellular localization of *Xenopus* Delta ligand.** *A*, schematic drawing of Mib2 constructs. *B*, requirement of both RING domains of Mib2 for the ubiquitination of XD. HEK-293A cells were co-transfected with RING mutant plasmid constructs. Cell lysates were immunoprecipitated (*IP*) with an anti-Myc antibody and detected with an anti-Ub antibody. The *top panel* shows the ubiquitination of XD by the Mib2 constructs, and the *bottom panel* is a blot showing the expression of the XD construct in cell lysates. *C*, subcellular localization of Mib2 (in *green*) and Notch ligands XD (in *red*). Mib2-GFP and/or Myc-tagged Notch ligand constructs were co-expressed in HeLa cells. Myc epitopes were detected with an anti-Myc antibody followed by a TRITC-labeled antibody. Nuclear DNA was stained with Hoechst (in *blue*). *a* and *b*, expression of XD-myc (*a* and *a′*) and Mib2-GFP (*b* and *b′*). *c*—*f*, co-transfection of XD-myc with various Mib2-GFP constructs, wild-type Mib2-GFP (*c*, *c′*, and *c″*), Mut1-GFP (*d*, *d′*, and *d″*), Mut2-GFP (*e*, *e′*, and *e″*), and Mut3-GFP (*f*, *f′*, and *f″*). *g*, co-transfection of XD-Δicd-myc with wild-type Mib2-GFP (*g*, *g′*, and *g″*). Overlapping expression is shown in *yellow*. Magnification: ×400. *IB*, immunoblot.

co-localized with Mib2-GFP (Fig. 4*C*, *c* and *c″*). These observations suggest that Mib2 promotes vesicular accumulation of Delta. When mutant Mib2-GFPs with mutations in the RING finger domain (Mut1, Mut2, and Mut3) were co-transfected with XD-myc in HeLa cells, none of these mutants were able to promote endocytosis of XD-myc (Fig. 4*C*, *d* and *d″*, *e* and *e″*, and *f* and *f″*). As expected, endocytosis of XD-Δicd was undetectable in the co-transfection of Mib2-GFP and XD-Δicd, which does not interact with Mib2. Thus, both the E3 ubiquitin ligase activity of Mib2 and the intracellular domain of XD are required for Delta endocytosis.

Mib2 Rescues the Neurogenic and Vasculogenic Phenotypes of Zebrafish mib^{ta52b} Mutants—Because Mib2 has biochemical similarities to Mib1, such as ligand binding, the ubiquitin

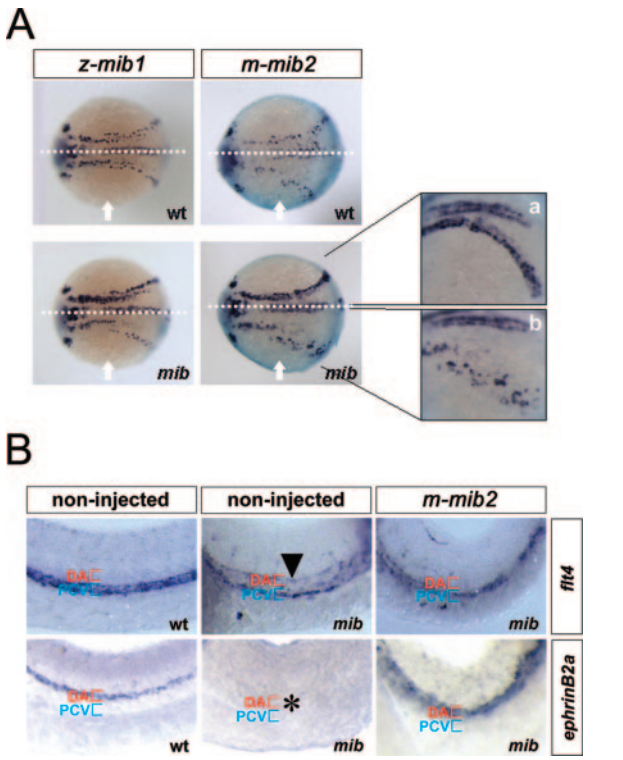

FIG. 5. **Rescues of neurogenic and vasculogenic phenotypes in zebrafish *mib*^{ta52b} mutants by mouse Mib2.** *A*, rescue of the neurogenic defect in the *mib*^{ta52b} mutants by Mib2. Zebrafish *mib1* (*z-mib1*, *left panels*) and mouse *mib2* (*m-mib2*, *right panels*) mRNA were injected on one side of zebrafish wild type (*wt*, *upper panels*) and *mib*^{ta52b} mutant (*mib*, *lower panels*) embryos at the two-cell stage, and *huC* (early neuronal cell marker) expression was examined at the 3-somite stage. *Arrows* indicate the injected side. *Dashed lines* indicate the border of the injected (*lower*) and non-injected (*upper*) side. The enlarged views (*a* and *b*) of *huC*-expressing cells in the non-injected side (*a*) and *mib2* mRNA-injected side (*b*) of *mib*^{ta52b} mutant embryos. Note the reduction of *huC*-expressing cells in the *mib2* mRNA-injected side. *B*, rescue of the vascular defect in the *mib*^{ta52b} mutants by Mib2. Mouse *mib2* mRNA was injected (*right panels*) in the one-cell stage of *mib*^{ta52b} mutant embryos, and the expression of *flt4* (venous vessel marker, *upper panels*) and *ephrinB2a* (arterial vessel marker, *lower panels*) was examined at the 30-somite stage. Note the restricted expression of *flt4* in the posterior cardinal vein (*upper right panel*) and the normal expression of *ephrinB2a* in the dorsal artery (*lower right panel*) of *mib*^{ta52b} mutants injected with the *mib2* mRNA. *DA*, dorsal artery; *PCV*, posterior cardinal vein. The *arrowhead* indicates the misexpression of *flt4* in DA of *mib*^{ta52b} mutant embryos and the *asterisk* indicates the loss of *ephrinB2a* in DA of *mib*^{ta52b} mutant embryos.

ligase activity, and the endocytic activity for Delta, we tested the possibility that Mib2 may rescue the defects in neurogenesis and vasculogenesis of the zebrafish *mib1* mutant, *mib*^{ta52b}.

The zebrafish *mib*^{ta52b} mutants exhibit massive neurogenesis, such as increased number of *huC* (early neuronal cell marker) expressing cells in neuroepithelium. Zebrafish embryos from *mib*^{ta52b} heterozygote intercrosses were injected in one side at the two-cell stage with mRNA encoding zebrafish Mib1 (positive control) or mouse Mib2, and their effects on neurogenesis were assayed by examining *huC* expression at the three-somite stage. The ectopic overexpression of zebrafish *mib1* reversed the massive *huC* expression in *mib*^{ta52b} mutants compared with its non-injected side (Fig. 5*A*, *left panel*). Interestingly, when mouse *mib2* mRNA was ectopically overexpressed in the *mib*^{ta52b} mutants, *huC* expression was also dramatically reduced as compared with that of the non-injected side (Fig. 5*A*, *right panel*). Enlarged views revealed a lower density of *huC*-expressing cells in the *mib2* mRNA-injected side in the *mib*^{ta52b} mutants, suggesting that Mib2 is able to generate Notch signaling to inhibit the neuronal fate in the neuroepithelium (Fig. 5*A*, *a* and *b*) (11).

The zebrafish *mib*^{ta52b} mutants also exhibited defects in arterial-venous differentiation, such as the loss of artery-specific markers and ectopic expression of venous markers within the dorsal aorta. The venous blood vessel marker *flt4* is ectopically expressed within the dorsal artery (DA) in *mib*^{ta52b} mutant embryos (Fig. 5*B*, *upper middle panel*) (23). When mouse *mib2* mRNA was injected in the one-cell stage of *mib*^{ta52b} mutant embryos, *flt4* became restricted to the posterior cardinal vein within the trunk at the 30-somite stage (Fig. 5*B*, *upper right panel*). In addition, when mouse *mib2* was ectopically overexpressed in zebrafish *mib*^{ta52b} mutants, the expression of the artery-specific marker, *ephrinB2a*, was normal, whereas uninjected mutant embryos failed to express *ephrinB2a* in the DA (Fig. 5*B*, *lower middle* and *right panels*). Taken together, these data suggest that Mib2 has functional similarities to Mib1.

Expression of mib1 and mib2—Despite the biochemical and functional similarities between Mib1 and Mib2, the zebrafish *mib*^{ta52b} mutants display severe defects in the Notch signaling pathway (11). Because mouse *mib2* mRNA injection into zebrafish *mib*^{ta52b} mutants rescued the neurogenic and vasculogenic defects, we speculated that zebrafish *mib2* (*z-mib2*) might not be expressed during embryonic stages. As expected, *z-mib2* is expressed at a very low level in 24 h post-fertilization zebrafish embryos, as compared with zebrafish *mib1* (*z-mib1*) (Fig. 6). Likewise, mouse *mib2* was slightly expressed in the tail bud and limb buds of E9.5 mouse embryos, and in the head region, tail bud, and limb buds of E10.5 mouse embryos, whereas mouse *mib1* mRNA was highly expressed in the head region, tail bud, limb buds, and somites of both E9.5 and E10.5 mouse embryos (Fig. 7, *A* and *B*). Interestingly, in the skin and intestine at postnatal day 1 (P1) and the adult intestine, *mib1* and *mib2* were expressed in similar patterns, in the hair follicles in the skin (Fig. 7, *C* and *D*) and the intestinal epithelium (Fig. 7, *E–H*). In the P1 neonatal intestine, however, *mib1* was highly expressed in the external muscle layer, whereas the expression of *mib2* was only slightly detected. Overall, *mib1* was highly expressed in both embryos and adult tissues, whereas *mib2* was highly expressed in neonates and adults, but only slightly in embryos, suggesting that *mib1* might have a dominant role during embryonic stages, and *mib1* and *mib2* might work cooperatively in neonates and adults.

DISCUSSION

Many E3 ubiquitin ligases are known to regulate Notch signaling (29). They are divided in two groups, one group that ubiquitinates Notch receptor and the other group that regulates Notch ligands. Sel-10 ubiquitinates the intracellular domain of Notch, and Itch cooperates with Numb to stimulate the endocytosis of Notch receptors (30, 31). Both Mind bomb and Neur ubiquitinate Delta and thus promote its endocytosis (11, 24, 25, 32). In the present study, we have cloned mouse Mib2, another homologous protein of zebrafish Mib1. Mib2 interacts with and ubiquitinates Delta. Moreover, it changes the subcellular localization of Delta to a vesicular compartment, suggesting the endocytosis of this protein. Importantly, it rescues the defects in neurogenesis and vasculogenesis of the zebrafish *mib*^{ta52b} mutants. Therefore, we concluded that Mib2 is another E3 ubiquitin ligase that targets the Notch ligand in the Notch signaling pathway.

Both mouse Mib1 and Mib2 have similar domain architectures, which consist of herc2/mib domains, a ZZ zinc finger, a mib repeat, ankyrin repeats, and RING domains. Two Mib homologues also exist in *Drosophila*, CG5841 and CG17492 (11). CG5841 has 3 RING finger domains, whereas CG17492

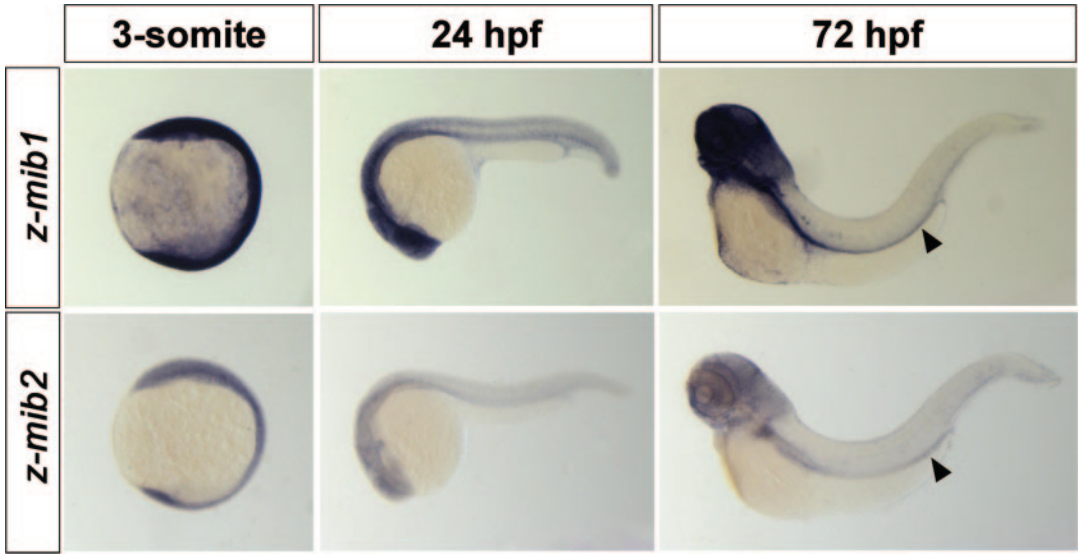

FIG. 6. **Expression of zebrafish *mib1* and *mib2*.** Whole mount *in situ* hybridization using zebrafish *mib1* (*z-mib1*, *upper panels*) and *mib2* (*z-mib2*, *lower panels*) antisense probes in the 3 somite, 24 h post-fertilization (*hpf*), and 72 hpf zebrafish embryos. Note that *z-mib1* is highly expressed throughout these stages, whereas *z-mib2* is expressed at very low levels. *Arrowheads* indicate the comparable expression levels of *z-mib1* and *z-mib2* in the 72 hpf embryos.

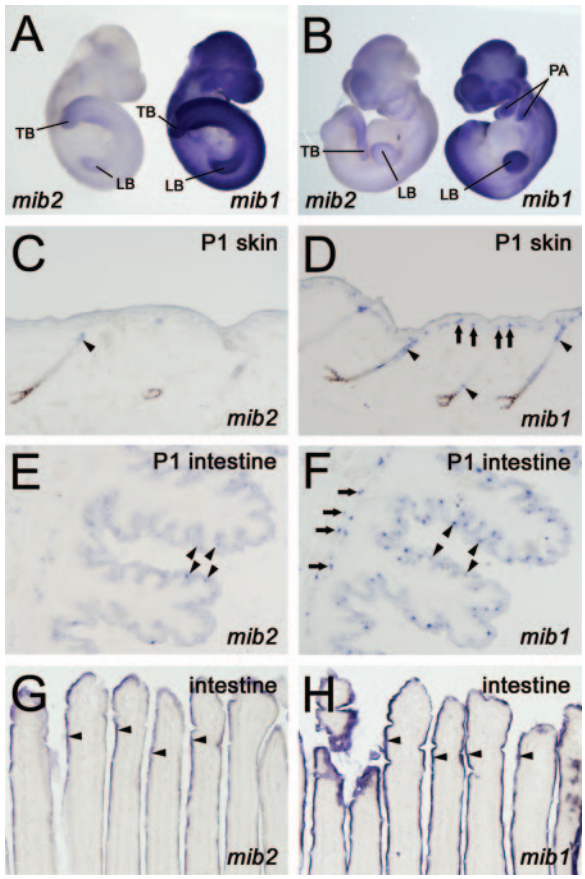

FIG. 7. **Expression of mouse *mib1* and *mib2*.** *A* and *B*, whole mount *in situ* hybridization using *mib2* (*left*) and *mib1* (*right*) antisense probes in E9.5 (*A*) and E10.5 (*B*) C57Bl/6 embryos. Note that *mib1* is broadly expressed throughout the body and highly expressed in the head region, pharyngeal arches (*PA*), presumptive limb buds (*LB*), tail bud (*TB*), and somites, whereas faint expression of *mib2* was detected in the head region, presumptive limb buds and tail bud. *C–H*, *in situ* hybridization using *mib2* (*C*, *E*, and *G*) and *mib1* (*D*, *F*, and *H*) antisense probes in the skin (P1 skin, *C* and *D*) and the intestine (*E–H*) sections from postnatal day 1 (P1 intestine, *E* and *F*) and 8 weeks (intestine, *G* and *H*). *Arrows* indicate the unique expression of *mib1* and *arrowheads* indicate the comparable expression of both *mib1* and *mib2*. Magnification: ×100.

has 2 RING finger domains (data not shown). They both have similar domain architecture as compared with those in rodents and human, indicating that Mib1 and Mib2 are evolutionarily conserved from fly to human. A comparison of the domain structures between Mib1 and Mib2 reveals that the RING finger domain is one of the characteristic features; there are three RINGs in Mib1 and two RINGs in Mib2, whereas most RING-type E3 ubiquitin ligases have only one RING finger domain.

Both Mib1 and Mib2 have RING finger domains at their C-terminal ends and the substrate-binding domain at their N-terminal ends. A classical RING finger domain is defined by a specific pattern of cysteine and histidine residues that are involved in zinc binding, which is important for the folding of the domain and its activity. RING fingers are classified as RING-H2 or RING-HC, depending on whether the fifth zinc-coordinating residue is a histidine (H2) or a cysteine (HC), respectively (33). Both Mib1 and Mib2 are the RING-HC type and have an E3 activity with E2 Ubc5a *in vitro* (11, 34). An *in vitro* ubiquitination assay revealed that the first RING finger in Mib2 is not essential for its self-ubiquitination. However, ubiquitination and endocytosis of XD by Mib2 require both RING finger domains, indicating that both are physiologically essential *in vivo*. The cooperative activity of the two RING finger domains has not been elucidated. Therefore, studies on the intermolecular mechanism that transfers ubiquitin from E2 to the Notch ligands by Mib1 and Mib2 will provide insights into the interesting domain-domain interactions.

There are five zebrafish *mib1* mutants (*tfi91*, *m178*, *m132*, *tfi101*, and *ta52b*) with mutations in the *mib1* locus. The *ta52b* mutants display more severe phenotypes than the other mutants (35). Three alleles of *mib1*, *tfi91*, *m178*, *and m132*, have a premature stop codon, and the other two, *tfi101* and *ta52b*, have point mutations in the RING domain (*ta52b*, M1013R; and *tfi101*, C1009S) (11). These findings raise the possibility that a point mutation in *ta52b* (Mib1-M1013R) could have dominant negative effects, which might be because of either blocking the wild type Mib1 that is translated from the maternal mRNA or blocking Mib2. Because *mib2* is weakly expressed or absent in the very early stages of embryogenesis and *mib1* is highly expressed maternally, it is more likely that Mib1-M1013R blocks the activity of the maternal Mib1 protein (11). When mouse *mib2* mRNA is

injected in the two-cell stage of *mib*^{ta52b} embryos, the ectopic overexpression of Mib2 might override the dominant negative effects of Mib1-M1013R and compensate for the defects in neurogenesis and artery formation.

The expression of Mib1 and Mib2 overlaps in many adult tissues, but is unique in others. Mib2 is highly expressed in adult tissues, such as heart, brain, liver, kidney, skin, and small intestine. We could not observe Mib2 expression in the muscle, which is inconsistent with a previous report (21). This discrepancy might be because of species difference between mouse and human. Mib1, also known as death-associated protein kinase-interacting protein (DIP-1), is expressed broadly in adult tissues but relatively highly in testis, ileum, and trachea (34). Consistently, we also observed high expression of Mib1 in testis, skin, and small intestine, but low expression in a broad range of other tissues (data not shown). These overlapping and unique expression patterns of Mib1 and Mib2 suggest that these two E3 ligases may work cooperatively, but sometimes independently in the regulation of Notch ligands. Notch signaling is critical for the maintenance and the differentiation of adult stem cells, such as hematopoietic stem cells, basal layer cells in the skin, and neural stem cells (36–38). Aberrant Notch signaling is also intimately involved in several cancers, such as pre-T cell acute lymphoblastic leukemias (39) and skin and corneal tumors (40). Many other human and mouse cancers, including certain neuroblastomas, and mammary, skin, cervical, and prostate cancers, are correlated with alterations in the Notch signaling pathways. Although the causal relationships await further characterization, these observations suggest broad roles for Notch dysfunction in cellular transformation, and both Mib1 and Mib2 might be involved in Notch signaling by regulating Notch ligands.

There are multiple Notch ligands, such as Delta and Serrate in *Drosophila*, four Delta homologues (Delta A, B, C, and D) and three Jagged homologues (Jag 1–3) in zebrafish, and three Delta-like ligands (Dll-1, -3, and -4) and Serrate-like ligands (Jagged-1 and -2) in mammals. For the regulation of these Notch ligands, two E3 regulators, Mib1 and Neur, have been identified so far. In the present study, we have identified a new E3 regulator, Mib2, that interacts with Delta and promotes its endocytosis through ubiquitination. Because the Notch signaling pathway is initiated when receptor-bearing cells interact with Notch ligands expressed by adjacent cells, we suggest that these three E3 ubiquitin-ligases might have critical roles in Notch activation, either cooperatively or independently.

Acknowledgments—We thank S. M. Kang for the ubiquitination assay and Y. J. Cho for purification of RING proteins.

REFERENCES

1. Sorkin, A., and Von Zastrow, M. (2002) *Nat. Rev. Mol. Cell. Biol.* **3,** 600–614
2. Kramer, H. (2000) *Science's STKE* http://stke.sciencemag.org/cgi/content/full/sigtrans;2000/53/PE1
3. Artavanis-Tsakonas, S., Matsuno, K., and Fortini, M. E. (1995) *Science* **268,** 225–232
4. Black, R. A., and White, J. M. (1998) *Curr. Opin. Cell Biol.* **10,** 654–659
5. Annaert, W., and De Strooper, B. (1999) *Trends Neurosci.* **22,** 439–443
6. Mumm, J. S., Schroeter, E. H., Saxena, M. T., Griesemer, A., Tian, X., Pan, D. J., Ray, W. J., and Kopan, R. (2000) *Mol. Cell* **5,** 197–206
7. Iso, T., Kedes, L., and Hamamori, Y. (2003) *J. Cell. Physiol.* **194,** 237–255
8. Nam, Y., Weng, A. P., Aster, J. C., and Blacklow, S. C. (2003) *J. Biol. Chem.* **278,** 21232–21239
9. Thomas, J. B., and Crews, S. T. (1990) *FASEB J.* **4,** 2476–2482
10. Baron, M. (2003) *Semin. Cell Dev. Biol.* **14,** 113–119
11. Itoh, M., Kim, C. H., Palardy, G., Oda, T., Jiang, Y. J., Maust, D., Yeo, S. Y., Lorick, K., Wright, G. J., Ariza-McNaughton, L., Weissman, A. M., Lewis, J., Chandrasekharappa, S. C., and Chitnis, A. B. (2003) *Dev. Cell* **4,** 67–82
12. Hrabe de Angelis, M., McIntyre, J., 2nd, and Gossler, A. (1997) *Nature* **386,** 717–721
13. Sidow, A., Bulotsky, M. S., Kerrebrock, A. W., Bronson, R. T., Daly, M. J., Reeve, M. P., Hawkins, T. L., Birren, B. W., Jaenisch, R., and Lander, E. S. (1997) *Nature* **389,** 722–725
14. Kusumi, K., Sun, E. S., Kerrebrock, A. W., Bronson, R. T., Chi, D. C., Bulotsky, M. S., Spencer, J. B., Birren, B. W., Frankel, W. N., and Lander, E. S. (1998) *Nat. Genet.* **19,** 274–278
15. Xue, Y., Gao, X., Lindsell, C. E., Norton, C. R., Chang, B., Hicks, C., Gendron-Maguire, M., Rand, E. B., Weinmaster, G., and Gridley, T. (1999) *Hum. Mol. Genet.* **8,** 723–730
16. Duarte, A., Hirashima, M., Benedito, R., Trindade, A., Diniz, P., Bekman, E., Costa, L., Henrique, D., and Rossant, J. (2004) *Genes Dev.* **18,** 2474–2478
17. Dunwoodie, S. L., Clements, M., Sparrow, D. B., Sa, X., Conlon, R. A., and Beddington, R. S. (2002) *Development* **129,** 1795–1806
18. Gale, N. W., Dominguez, M. G., Noguera, I., Pan, L., Hughes, V., Valenzuela, D. M., Murphy, A. J., Adams, N. C., Lin, H. C., Holash, J., Thurston, G., and Yancopoulos, G. D. (2004) *Proc. Natl. Acad. Sci. U. S. A.* **101,** 15949–15954
19. Jiang, R., Lan, Y., Chapman, H. D., Shawber, C., Norton, C. R., Serreze, D. V., Weinmaster, G., and Gridley, T. (1998) *Genes Dev.* **12,** 1046–1057
20. Krebs, L. T., Shutter, J. R., Tanigaki, K., Honjo, T., Stark, K. L., and Gridley, T. (2004) *Genes Dev.* **18,** 2469–2473
21. Takeuchi, T., Heng, H. H., Ye, C. J., Liang, S. B., Iwata, J., Sonobe, H., and Ohtsuki, Y. (2003) *Am. J. Pathol.* **163,** 1395–1404
22. Kim, C. H., Ueshima, E., Muraoka, O., Tanaka, H., Yeo, S. Y., Huh, T. L., and Miki, N. (1996) *Neurosci. Lett.* **216,** 109–112
23. Lawson, N. D., Scheer, N., Pham, V. N., Kim, C. H., Chitnis, A. B., Campos-Ortega, J. A., and Weinstein, B. M. (2001) *Development* **128,** 3675–3683
24. Lai, E. C., Deblandre, G. A., Kintner, C., and Rubin, G. M. (2001) *Dev. Cell* **1,** 783–794
25. Pavlopoulos, E., Pitsouli, C., Klueg, K. M., Muskavitch, M. A., Moschonas, N. K., and Delidakis, C. (2001) *Dev. Cell* **1,** 807–816
26. Pfeffer, S. (2003) *Cell* **112,** 507–517
27. Aguilar, R. C., and Wendland, B. (2003) *Curr. Opin. Cell Biol.* **15,** 184–190
28. Hicke, L. (1997) *FASEB J.* **11,** 1215–1226
29. Lai, E. C. (2002) *Curr. Biol.* **12,** R74–R78
30. McGill, M. A., and McGlade, C. J. (2003) *J. Biol. Chem.* **278,** 23196–23203
31. Wu, G., Lyapina, S., Das, I., Li, J., Gurney, M., Pauley, A., Chui, I., Deshaies, R. J., and Kitajewski, J. (2001) *Mol. Cell. Biol.* **21,** 7403–7415
32. Deblandre, G. A., Lai, E. C., and Kintner, C. (2001) *Dev. Cell* **1,** 795–806
33. Fang, S., Lorick, K. L., Jensen, J. P., and Weissman, A. M. (2003) *Semin. Cancer Biol.* **13,** 5–14
34. Jin, Y., Blue, E. K., Dixon, S., Shao, Z., and Gallagher, P. J. (2002) *J. Biol. Chem.* **277,** 46980–46986
35. Haddon, C., Jiang, Y. J., Smithers, L., and Lewis, J. (1998) *Development* **125,** 4637–4644
36. Hitoshi, S., Alexson, T., Tropepe, V., Donoviel, D., Elia, A. J., Nye, J. S., Conlon, R. A., Mak, T. W., Bernstein, A., and van der Kooy, D. (2002) *Genes Dev.* **16,** 846–858
37. Moore, K. A. (2004) *Curr. Opin. Hematol.* **11,** 107–111
38. Thelu, J., Rossio, P., and Favier, B. (2002) *BMC Dermatol.* **2,** 7
39. Ellisen, L. W., Bird, J., West, D. C., Soreng, A. L., Reynolds, T. C., Smith, S. D., and Sklar, J. (1991) *Cell* **66,** 649–661
40. Nicolas, M., Wolfer, A., Raj, K., Kummer, J. A., Mill, P., van Noort, M., Hui, C. C., Clevers, H., Dotto, G. P., and Radtke, F. (2003) *Nat. Genet.* **33,** 416–421